

# Rotordynamic Coefficients in Staggered Labyrinth Seals

Dursun Eser\*, Yilmaz Dereli

Mathematics Department, Science and Art Faculty, Osmangazi University,  
26480 Eskişehir Turkey

In this paper, the flow properties of staggered labyrinth seals are investigated. Leakage flowrates and pressure distributions are calculated for this seal. Then the dynamic stiffness and damping coefficients are calculated. The results are compared to the results of the some other papers.

**Key Words :** Staggered Labyrinth Seal, Rotordynamic Coefficient, Perturbation Analysis

## Nomenclature

$A$  : Circumferential transverse surface area  
 $ANAR$  : Circumferential clearance area of seal  
 $a_r, a_s$  : Dimensionless length upon which shear stress acts  
 $B$  : Height of seal stript  
 $C, c$  : Direct and cross-coupled damping coefficients  
 $Cr$  : Radial clearance  
 $D$  : Step height  
 $Dh$  : Hydraulic diameter  
 $K, k$  : Direct and cross-coupled stiffness coefficients  
 $L$  : Pitch of seal stript  
 $\dot{m}$  : Leakage mass flow  
 $m, n$  : Coefficients for friction factor  
 $NT$  : Number of teeth  
 $P$  : Pressure  
 $\dot{q}$  : Leakage mass flow per area  
 $R$  : Gas constant  
 $R_s$  : Seal radius  
 $T$  : Temperature  
 $TIPLN$  : Tooth tip width

$V$  : Circumferential velocity  
 $\omega$  : Shaft angular velocity  
 $\varepsilon$  : Eccentricity ratio  
 $\gamma$  : Ratio of specific heats  
 $\mu_{1i}$  : Contraction coefficient  
 $\mu_{2i}$  : Kinetic energy carry-over coefficient  
 $\nu$  : Kinematic viscosity  
 $\theta$  : Angular coordinate  
 $\rho$  : Density  
 $\tau_r$  : The shear stress of the rotor surface  
 $\tau_s$  : The shear stress of the stator surface

## Subscripts

0, 1 : Zeroth and first-order perturbations  
 $r, s$  : Rotor, stator  
 $i$  :  $i$ -th cavity

## 1. Introduction

Labyrinth seals are used in turbines and compressors as well as in some pumps. The primary objective of labyrinth seal is to control fluid leakage. There are a few types of labyrinth seals are being used. The most common one is the straight through labyrinth seals which were studied by Eser and Kazakia (1995), Childs and Scharrer (1986), Dillon (1991) etc. The next common seals are stepped labyrinth seals which were studied by Scharrer (1989), Ha (2001), Eser (2002). Staggered labyrinth seals are another type of seals which is the main subject of this study.

\* Corresponding Author.

E-mail : deser@ogu.edu.tr

TEL : +90-222-2290433/2233;

FAX : +90-222-2293578

Mathematics Department, Science and Art Faculty, Osmangazi University, 26480 Eskişehir Turkey. (Manuscript Received May 16, 2003; Revised February 17, 2004)

Here we present an analysis for the staggered labyrinth gas seals shown in Fig 1. The continuity and momentum equation are derived for single control volumes shown in Fig. 2.

The first order equations are linearized using a perturbation analysis for small motion about a centered position. The resulting set of linear algebraic equations are solved by using a numerical method for the pressure and velocity perturbations. The rotor dynamic coefficients are

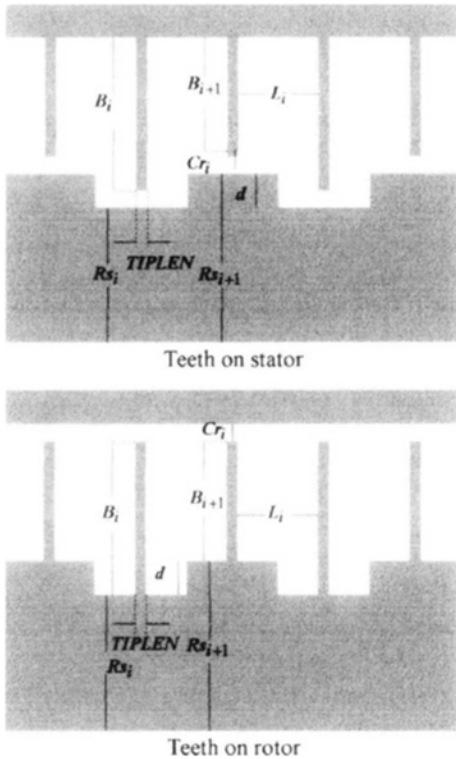


Fig. 1 Geometric details in staggered labyrinth seal

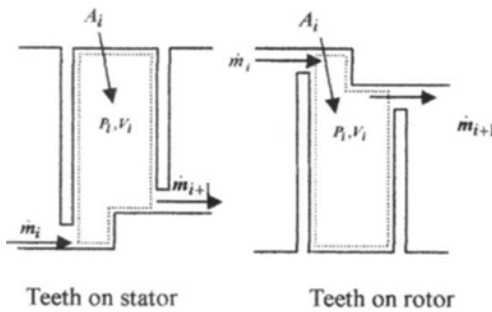


Fig. 2 Control volumes

obtained by integrating the pressure perturbations around the shaft.

### 2. Procedure

The Neuman’s leakage model is used to calculate the leakage flowrate which is given as

$$\dot{m} = \mu_{1i} \mu_{2i} \frac{ANAR_i}{\sqrt{RT}} \sqrt{P_{i-1}^2 - P_i^2} \quad (1)$$

The zeroth order continuity equation implies that leakage flowrates are equal in each cavities, i.e.

$$\dot{m}_1 = \dot{m}_2 = \dots = \dot{m}_{NT} = \dot{m} \quad (2)$$

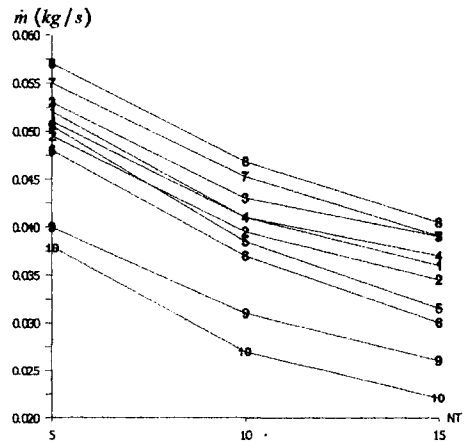
We have compared the leakage flowrate results to the results of Scharrer (1989) and Ha (2001). This comparison is given in Fig. 3 and it is satisfactory.

The circumferential momentum equation can be written for ith labyrinth cavity as

$$\dot{m} (V_i - V_{i-1}) = 2\pi (\tau_{ri} a_{ri} - \tau_{si} a_{si}) \quad (3)$$

where the shear stress at the stator surface area is

$$\tau_{si} = 0.5 \rho_i V_i^2 n_s \left( \frac{|V_i| Dh_i}{\nu} \right)^{ms} \quad (4)$$



$d = 0.001, P_N = 7.00E + 5, WRPM = 2000C$

Fig. 3 Comparison of leakage flowrate to the results of Scharrer (1989) and Ha (2001)

and at the rotor surface area is

$$\tau_r = 0.5 \rho_i (R_{s_i} \omega - V_i)^2 n r \left( \frac{|R_{s_i} \omega - V_i| Dh_i}{\nu} \right)^{m r} \quad (5)$$

The velocity distribution is given in Fig. 4 for teeth on stator and teeth on rotor. The seal geometries, the seal conditions and the labyrinth seal types used here are given Table 1.

**Table 1** Seal geometries and operating conditions and labyrinth seal types

NT=5, 10, 15	$P_{IN}=7.00E+5, 3.08E+5 \text{ Nm}^2$
$d=0.00025, 0.00100 \text{ m}$	$P_{OUT}=1.01E+5 \text{ Nm}^2$
$V(0)=60 \text{ m/s}$	$W=16000, 20000 \text{ rpm}$
$RS(1)=0.0756 \text{ m}$	$L(1)=0.002175, 0.003175 \text{ m}$
$B(1)=0.003175 \text{ m}$	$T=300 \text{ }^\circ\text{K}$
$Cr(1)=0.000127 \text{ m}$	$R=287.06 \text{ Nm/kg}^\circ\text{K}$
$TIPLN=.2E-4 \text{ m}$	Fluid : Air

- 1 : straight labyrinth seal teeth on stator
- 2 : straight labyrinth seal teeth on rotor
- 3 : diverging stepped labyrinth seal teeth on stator
- 4 : diverging stepped labyrinth seal teeth on rotor
- 5 : converging stepped labyrinth seal teeth on stator
- 6 : converging stepped labyrinth seal teeth on rotor
- 7 : staggered labyrinth seal teeth on stator
- 8 : staggered labyrinth seal teeth on rotor
- 9 : diverging stepped labyrinth seal teeth on rotor
- 10 : converging stepped labyrinth seal teeth on rotor (Ha, 2001)

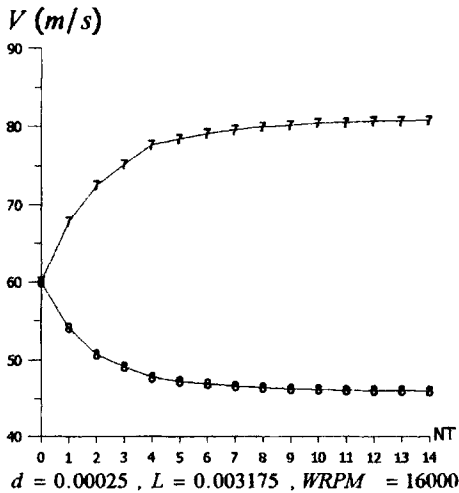


**Fig. 4** Velocity distribution

### 3. Governing Equations

Using the control volume in Fig. 5, the continuity equation can be derived as

$$\frac{\partial}{\partial t}(\rho_i A_i) + \frac{\rho_i V_i}{R_{s_i}} \frac{\partial A_i}{\partial \theta} + \frac{\rho_i A_i}{R_{s_i}} \frac{\partial V_i}{\partial \theta} + \frac{A_i V_i}{R_{s_i}} \frac{\partial \rho_i}{\partial \theta} + \dot{q}_{i+1} \frac{R_{s_{i+1}}}{R_{s_i}} - \dot{q}_i = 0 \quad (6)$$

where

$$A_i = (B_{i+1} + Cr_i) L_i + \frac{dL_i}{2} = \left( B_{i+1} + Cr_i + \frac{d}{2} \right) L_i \quad (7)$$

is the transverse surface area. Height of seal strip  $B_i$  and seal radius  $R_{s_i}$  change at each cavity and these are defined as

$$B_{i+1} = B_i + (-1)^i d \quad (8)$$

$$R_{s_{i+1}} = R_{s_i} + (-1)^{i+1} d \quad (9)$$

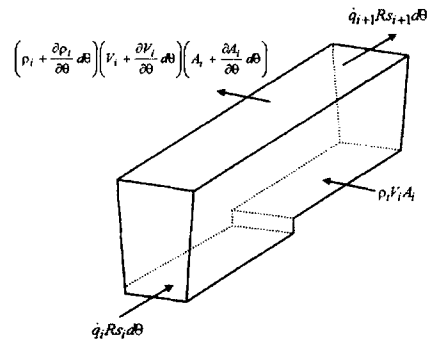


**Fig. 5** Control volume used to derive the continuity equation

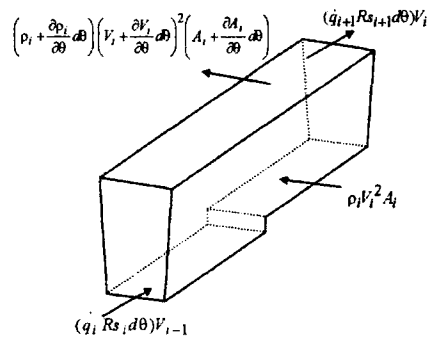


**Fig. 6** Control volume used to derive the momentum equation

Using the control volume in Fig. 6, the momentum equation is derived as

$$\begin{aligned} \frac{\partial}{\partial t}(\rho_i V_i A_i) = & -\frac{\rho_i V_i^2}{R_{S_i}} \frac{\partial A_i}{\partial \theta} - \frac{V_i^2 A_i}{R_{S_i}} \frac{\partial \rho_i}{\partial \theta} \\ & - \frac{2\rho_i A_i V_i}{R_{S_i}} \frac{\partial V_i}{\partial \theta} + \dot{q}_i V_{i-1} - \dot{q}_{i+1} \frac{R_{S_{i+1}}}{R_{S_i}} V_i \quad (10) \\ & - \frac{A_i}{R_{S_i}} \frac{\partial P_i}{\partial \theta} + \tau_{ri} a_{ri} - \tau_{si} a_{si} \end{aligned}$$

where the dimensionless shear stress lengths for teeth on stator are defined as

$$a_{si} = B_i + B_{i+1} + L_i \quad (11)$$

$$a_{ri} = L_i + d \quad (12)$$

and shear stress lengths for teeth on rotor are defined as

$$a_{ri} = B_i + B_{i+1} + L_i \quad (13)$$

$$a_{si} = L_i + d \quad (14)$$

Multiplying the continuity Eq. (6) with the circumferential velocity  $V_i$  and subtracting from the momentum Eq. (10) we obtain the simpler momentum equation as

$$\begin{aligned} \rho_i A_i \frac{\partial V_i}{\partial t} = & -\frac{\rho_i V_i A_i}{R_{S_i}} \frac{\partial V_i}{\partial \theta} - \dot{q}_i (V_i - V_{i-1}) \quad (15) \\ & - \frac{A_i}{R_{S_i}} \frac{\partial \rho_i}{\partial \theta} + \tau_{ri} a_{ri} - \tau_{si} a_{si} \end{aligned}$$

The leakage equation

$$\dot{q}_i = \mu_{1i} \mu_{2i} H_i \sqrt{\frac{P_{i-1}^2 - P_i^2}{RT}} \quad (16)$$

is used to calculate the leakage flowrate and pressure distributions in cavities of labyrinth seals. The flow coefficient  $\mu_{1i}$  and kinetic energy carryover coefficient  $\mu_{2i}$  are same as in Childs and Scharrer (1986).

### 4. First Order Solutions

We use the perturbation analysis to linearize the continuity and circumferential momentum equations. The perturbation parameters used here are

$$P_i = P_{0i} + \varepsilon P_{1i}(t, \theta) + \dots \quad (17)$$

$$V_i = V_{0i} + \varepsilon V_{1i}(t, \theta) + \dots \quad (18)$$

$$\dot{q}_i = \dot{q}_{0i} + \varepsilon \dot{q}_{1i}(t, \theta) + \dots \quad (19)$$

$$\dot{\tau}_{si} = \dot{\tau}_{s0i} + \varepsilon \dot{\tau}_{s1i}(t, \theta) + \dots \quad (20)$$

$$\dot{\tau}_{ri} = \dot{\tau}_{r0i} + \varepsilon \dot{\tau}_{r1i}(t, \theta) + \dots \quad (21)$$

$$\mu_i = \mu_{0i} + \varepsilon \mu_{1i}(t, \theta) + \dots \quad (22)$$

The radial clearance variation which is produced by such a disturbance is expanded in the form

$$\begin{aligned} H_i = & H_{0i} + \varepsilon H_{1i}(t, \theta) + \dots \quad (23) \\ = & C r_i + \varepsilon H_{1i}(t, \theta) + \dots \end{aligned}$$

where  $\varepsilon = e/Cr_i$  is the eccentricity ratio. Substituting these parameters in the continuity equation and neglecting the terms of  $\varepsilon^2$  and higher, we get the first order continuity equation for the  $i$ -th cavity as

$$\begin{aligned} G_{1i} \frac{\partial P_{1i}}{\partial t} + G_{1i} \frac{V_{0i}}{R_{S_i}} \frac{\partial P_{1i}}{\partial \theta} + G_{1i} \frac{P_{0i}}{R_{S_i}} \frac{\partial V_{1i}}{\partial \theta} \\ + G_{3i} P_{1i} + G_{4i} P_{1i+1} + G_{5i} P_{1i-1} \quad (24) \\ = -G_{6i} H_{1i} - G_{2i} \frac{\partial H_{1i}}{\partial t} - G_{2i} \frac{V_{0i}}{R_{S_i}} \frac{\partial H_{1i}}{\partial \theta} \end{aligned}$$

where the coefficients  $G_i$ 's are given in Appendix A.

Substituting the same perturbation parameters into the circumferential momentum equation we obtain the first order momentum equation as

$$\begin{aligned} X_{1i} \left( \frac{\partial V_{1i}}{\partial t} + \frac{V_{0i}}{R_{S_i}} \frac{\partial V_{1i}}{\partial \theta} \right) + \frac{A_{0i}}{R_{S_i}} \frac{\partial P_{1i}}{\partial \theta} \\ + X_{2i} V_{1i} - \dot{q}_{0i} V_{1i-1} + X_{3i} P_{1i} + X_{4i} P_{1i-1} \quad (25) \\ = X_{5i} H_{1i} \end{aligned}$$

where the coefficients  $X_i$ 's are given in Appendix A.

Eqs. (24) ~ (25) can be reduced to the following system of linear algebraic equations

$$\begin{aligned} [A_i^{-1}] \{ Y_{i-1} \} + [A_i^0] \{ Y_i \} + [A_i^+] \{ Y_{i+1} \} \\ = [a \{ B_i \} + b \{ C_i \}] \quad (26) \end{aligned}$$

where  $Y_i$ 's and the A matrices and column vectors B and C are given in Appendix B.

The solution of above system is

$$\{ P_i \} = a \{ F_{ai} \} + b \{ F_{bi} \} \quad (27)$$

where  $P_i$  and  $F_i$ 's are defined as

$$\{P_{1i}\} = [P_{ci}^+, P_{si}^+, P_{ci}^-, P_{si}^-]^T \quad (28)$$

$$\{F_{ai}\} = [F_{aci}^+, F_{asi}^+, F_{aci}^-, F_{asi}^-]^T \quad (29)$$

$$\{F_{bi}\} = [F_{bci}^+, F_{bsi}^+, F_{bci}^-, F_{bsi}^-]^T \quad (30)$$

Using these in Eq. (27) we get

$$P_{ci}^+ = aF_{aci}^+ + bF_{bsi}^- \quad (31)$$

$$P_{si}^+ = aF_{asi}^+ + bF_{bsi}^- \quad (32)$$

$$P_{ci}^- = aF_{aci}^- + bF_{bci}^- \quad (33)$$

$$P_{si}^- = aF_{asi}^- + bF_{bsi}^- \quad (34)$$

These are to be used in calculation of rotordynamic coefficients.

### 5. Calculation of Rotordynamic Coefficients

Direct and cross coupled stiffness coefficients  $K$  and  $k$ , damping coefficients  $C$  and  $c$  are given by Childs and Scharrer (1986) as

$$K = \pi \sum_{i=1}^{NC} R_{Si} L_i (F_{aci}^+ + F_{aci}^-) \quad (35)$$

$$k = \pi \sum_{i=1}^{NC} R_{Si} L_i (F_{bsi}^+ + F_{bsi}^-) \quad (36)$$

$$C = \frac{\pi}{\Omega} \sum_{i=1}^{NC} R_{Si} L_i (F_{asi}^+ + F_{asi}^-) \quad (37)$$

$$c = \frac{\pi}{\Omega} \sum_{i=1}^{NC} R_{Si} L_i (F_{bci}^+ + F_{bci}^-) \quad (38)$$

These coefficients are calculated by using the solution parameters of pressure distribution in the first order solution.

### 6. Results

The geometry and the operating conditions used here are given in Table 2. These geometry and conditions are taken from Eser and Kazakia (1995), Eser (2002). Here we use staggered labyrinth seal types whose teeth on stator and on the rotor. These seal types are given in Fig. 1. We compare our results to the results of Eser and Kazakia (1995), Eser (2002) using the cases in Table 2. The comparison of rotordynamic coefficients are given in Figs. 7~10 for the first three cases of Table 2. We compare the rotordynamic coefficients for straight and staggered labyrinth seals teeth on rotor. These comparisons

**Table 2** The geometry and the operating conditions for four different cases

Definition of cases	Case 1	Case 2	Case 3	Case 4
$P_{IN}$ (bar)	3.08	5.84	8.22	3.08
$P_{OUT}$ (bar)	1.01	1.01	1.01	1.01
$V_0$ (m/s)	60	60	60	60
$w$ (rpm)	16000	9000	6000	16000
$Cr$ (mm)	0.33	0.33	0.33	0.33
$Rs$ (mm)	75.6	75.6	75.6	75.6
$B$ (mm)	3.175	3.175	3.175	3.175
$L$ (mm)	3.175	3.175	3.175	3.175
$d$ (mm)	0.25	0.25	0.25	0.25, 0.50, 0.75, 1.00
No. of teeth	16	16	16	16
Teeth on	Stator	Stator	Stator	Stator, Rotor
$TIPL EN$	.2E-4	.2E-4	.2E-4	.2E-4

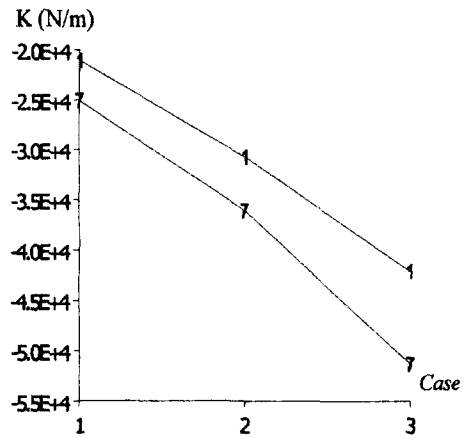


**Fig. 7** Direct stiffness coefficient

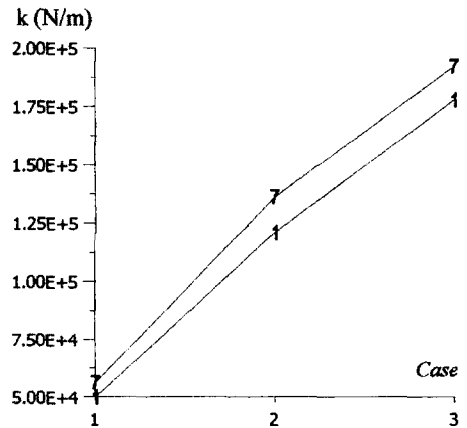


**Fig. 8** Cross coupled stiffness coefficient

are satisfactory. Using the case 4 with different step sizes we give the comparison of rotordynamic

coefficients in Figs. 11~14. These comparisons are reasonable.

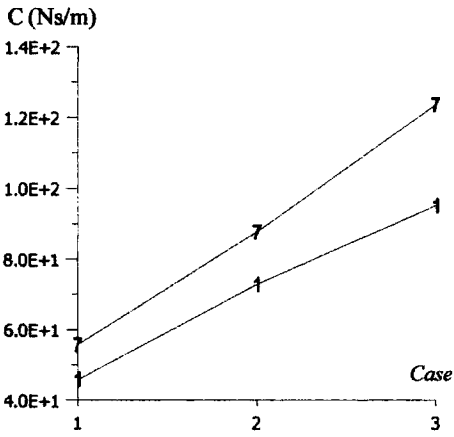


Fig. 9 Direct damping coefficient

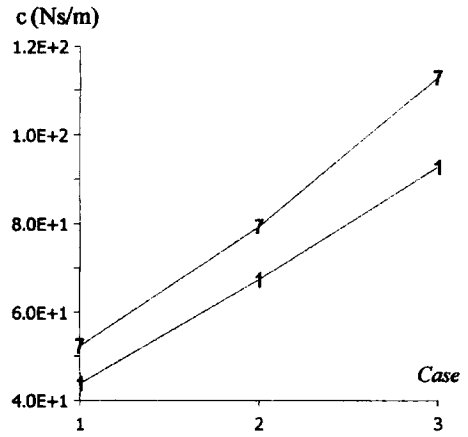


Fig. 10 Cross coupled damping coefficient

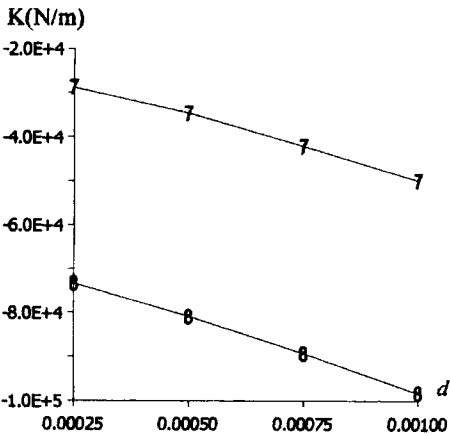


Fig. 11 Direct stiffness coefficient

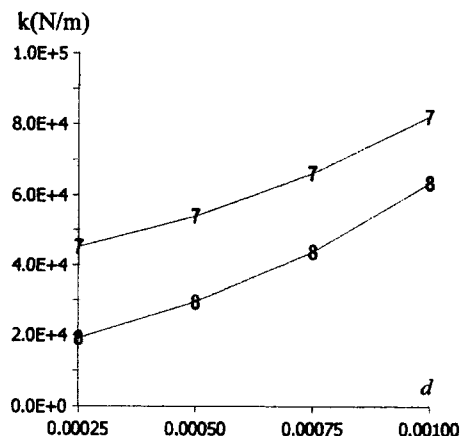


Fig. 12 Cross coupled stiffness coefficient

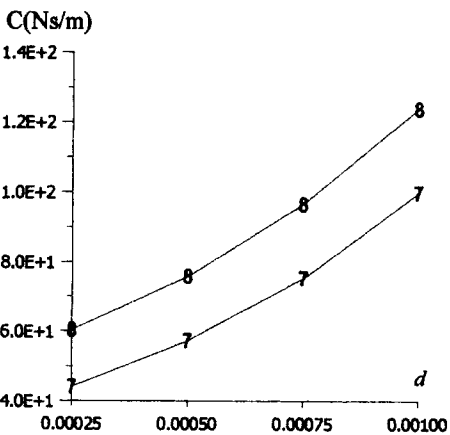


Fig. 13 Direct damping coefficient

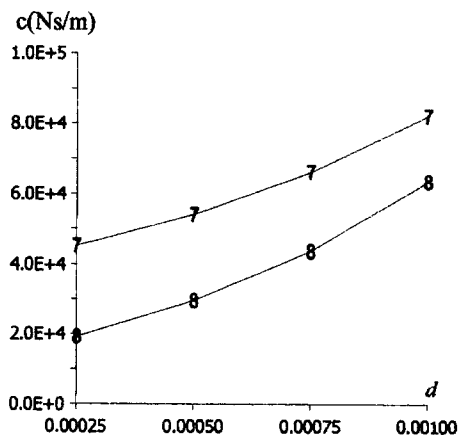


Fig. 14 Cross coupled damping coefficient

**References**

Childs, D. W. and Scharrer, J. K., 1986, "An Iwatsubo-based Solution for Labyrinth Seals: Comparison to Experimental Results," *Journal of Engineering for Gas Turbines and Power*, Vol. 108, pp. 325~331.

Dillon, J. L., 1990, "A Study of Turbomachinery Compressible Gas Labyrinth Seal Rotordynamic Coefficients," Ms. Thesis, Lehigh University.

Eser, D. and Kazakia, J. K., 1995, "Air Flow in Cavities of Labyrinth Seals," *International Journal of Engineering Science*, Vol. 33, No. 15, pp. 2309~2326.

Eser, D., 2002, "Rotordynamic Coefficients in Stepped Labyrinth Seals," *Computer Methods in Applied Mechanics and Engineering*, Vol. 191, Issues: 29~30, pp. 3127~3135.

Ha, T. W., 2001, "Rotordynamic Analysis for Stepped-Labyrinth Gas Seals Using Moody's Friction-Factor Model," *KSME International Journal*, Vol. 15, pp. 1217~1225.

Scharrer, J. K., 1989, "Rotordynamic Coefficients for Stepped Labyrinth Gas Seals," *Journal of Tribology*, Vol. 111, pp. 101~107.

**Appendix A**

The coefficients  $G_i$ 's are

$$G_{1i} = \frac{A_{0i}}{RT}, \quad G_{2i} = \frac{P_{0i}L_i}{RT}$$

$$G_{3i} = \frac{RS_{i+1}}{RS_i} \frac{\dot{q}_{0i+1}\mu_{0i+1}}{\pi} (5-4S_{0i+1}) \left(\frac{\gamma-1}{\gamma}\right) \left(\frac{1}{P_{0i+1}}\right)^{\frac{1}{\gamma}} + \frac{RS_{i+1}}{RS_i} \frac{\dot{q}_{0i+1}P_{0i}}{P_{0i}^2 - P_{0i+1}^2} + \dot{q}_{0i} \frac{P_{0i}}{P_{0i}^2 - P_{0i}^2}$$

$$+ \frac{\dot{q}_{0i}\mu_{0i}}{\pi} (5-4S_{0i}) \left(\frac{\gamma-1}{\gamma}\right) \left(\frac{1}{P_{0i}}\right) \left(\frac{P_{0i-1}}{P_{0i}}\right)^{\frac{\gamma-1}{\gamma}}$$

$$G_{4i} = \frac{RS_{i+1}}{RS_i} \frac{\dot{q}_{0i+1}\mu_{0i+1}}{\pi} (4S_{0i+1}-5) \left(\frac{\gamma-1}{\gamma}\right) \left(\frac{1}{P_{0i+1}}\right) \left(\frac{P_{0i}}{P_{0i+1}}\right)^{-\frac{1}{\gamma}} - \frac{RS_{i+1}}{RS_i} \frac{\dot{q}_{0i+1}}{P_{0i}^2 - P_{0i+1}^2}$$

$$G_{5i} = \frac{\dot{q}_{0i}\mu_{0i}}{\pi} (4S_{0i}-5) \left(\frac{\gamma-1}{\gamma}\right) \left(\frac{1}{P_{0i}}\right) \left(\frac{P_{0i-1}}{P_{0i}}\right)^{\frac{\gamma-1}{\gamma}} - \dot{q}_{0i} \frac{P_{0i}}{P_{0i-1}^2 - P_{0i}^2}$$

$$G_{6i} = \frac{RS_{i+1}}{RS_i} \frac{\dot{q}_{0i+1}}{Cr_{i+1}} - \frac{\dot{q}_{0i}}{Cr_i}$$

The coefficients  $X_i$ 's are

$$X_{1i} = \frac{P_{0i}A_{0i}}{RT}$$

$$X_{2i} = \dot{q}_{0i} + \frac{(2+mS)\tau_{s0i}a_{si}}{V_{0i}} + \frac{(2+m\tau)\tau_{r0i}a_{rsi}}{(RS_iW - V_{0i})}$$

$$X_{3i} = \frac{\tau_{s0i}a_{si}}{P_{0i}} - \frac{\tau_{r0i}a_{ri}}{P_{0i}} + \frac{\dot{q}_{0i}\mu_{0i}}{\pi} (4S_{0i}-5) \left(\frac{\gamma-1}{\gamma}\right) \left(\frac{1}{P_{0i}}\right) \left(\frac{P_{0i-1}}{P_{0i}}\right)^{\frac{\gamma-1}{\gamma}} (V_{0i} - V_{0i-1}) - \dot{q}_{0i} \frac{P_{0i}}{P_{0i-1}^2 - P_{0i}^2} (V_{0i} - V_{0i-1})$$

$$X_{4i} = -\frac{\dot{q}_{0i}\mu_{0i}}{\pi} (4S_{0i}-5) \left(\frac{\gamma-1}{\gamma}\right) \left(\frac{1}{P_{0i-1}}\right) \left(\frac{P_{0i-1}}{P_{0i}}\right)^{-\frac{1}{\gamma}} (V_{0i} - V_{0i-1}) + \dot{q}_{0i} \frac{P_{0i-1}}{P_{0i-1}^2 - P_{0i}^2} (V_{0i} - V_{0i-1})$$

$$X_{5i} = -\frac{\dot{q}_{0i}}{Cr_i} (V_{0i} - V_{0i-1}) - \frac{mS\tau_{s0i}a_{si}Dh_{0i}(d+2L_i)}{L_i(2B_{i+1} + Cr_i + d)^2} + \frac{m\tau\tau_{r0i}a_{ri}Dh_{0i}(d+2L_i)}{L_i(2B_{i+1} + Cr_i + d)^2}$$

Hydraulic diameter  $Dh_i$  is defined as

$$Dh_i = \frac{(2B_{i+1} + 2Cr_i + d)L_i}{B_{i+1} + Cr_i + d + L_i}$$

**Appendix B**

$$\{Y_{i-1}\} = \left\{ \frac{P_{1i-1}}{V_{1i-1}} \right\}, \{Y_i\} = \left\{ \frac{P_i}{V_i} \right\}, \{Y_{i+1}\} = \left\{ \frac{P_{i+1}}{V_{i+1}} \right\}$$

$$\{B_i\} = \left\{ \frac{\hat{B}_i}{\hat{B}_i} \right\}, \{C_i\} = \left\{ \frac{\hat{C}_i}{\hat{C}_i} \right\}$$

$$\hat{B}_i = \left[ \frac{G_{6i}}{2}, \frac{G_{2i}}{2} \left( \frac{V_{0i}}{RS_i} + \Omega \right), \frac{-G_{6i}}{2}, \frac{-G_{2i}}{2} \left( \frac{V_{0i}}{RS_i} - \Omega \right) \right]^T$$

$$\hat{C}_i = \left[ \frac{G_{6i}}{2}, \frac{-G_{2i}}{2} \left( \frac{V_{0i}}{RS_i} + \Omega \right), \frac{G_{6i}}{2}, \frac{-G_{2i}}{2} \left( \frac{V_{0i}}{RS_i} - \Omega \right) \right]^T$$

$$\hat{\hat{B}}_i = \left[ \frac{-X_{5i}}{2}, 0, \frac{-X_{5i}}{2}, 0 \right]^T, \hat{\hat{C}}_i = \left[ \frac{-X_{5i}}{2}, 0, \frac{-X_{5i}}{2}, 0 \right]^T$$

$$A_i^{-1} = \begin{bmatrix} G_{5i} & 0 & 0 & 0 & 0 & 0 & 0 & 0 \\ 0 & G_{5i} & 0 & 0 & 0 & 0 & 0 & 0 \\ 0 & 0 & G_{5i} & 0 & 0 & 0 & 0 & 0 \\ 0 & 0 & 0 & G_{5i} & 0 & 0 & 0 & 0 \\ X_{4i} & 0 & 0 & 0 & -\dot{q} & 0 & 0 & 0 \\ 0 & X_{4i} & 0 & 0 & 0 & -\dot{q} & 0 & 0 \\ 0 & 0 & X_{4i} & 0 & 0 & 0 & -\dot{q} & 0 \\ 0 & 0 & 0 & X_{4i} & 0 & 0 & 0 & -\dot{q} \end{bmatrix} \quad A_i^{+1} = \begin{bmatrix} G_{4i} & 0 & 0 & 0 & 0 & 0 & 0 & 0 \\ 0 & G_{4i} & 0 & 0 & 0 & 0 & 0 & 0 \\ 0 & 0 & G_{4i} & 0 & 0 & 0 & 0 & 0 \\ 0 & 0 & 0 & G_{4i} & 0 & 0 & 0 & 0 \\ 0 & 0 & 0 & 0 & 0 & 0 & 0 & 0 \\ 0 & 0 & 0 & 0 & 0 & 0 & 0 & 0 \\ 0 & 0 & 0 & 0 & 0 & 0 & 0 & 0 \\ 0 & 0 & 0 & 0 & 0 & 0 & 0 & 0 \end{bmatrix}$$

$$A_{\theta} = \begin{bmatrix} G_{3i} & G_{1i}\left(\Omega + \frac{V_{\theta i}}{RS_i}\right) & 0 & 0 & 0 & G_{1i} \frac{P_{\theta i}}{RS_i} & 0 & 0 \\ -G_{1i}\left(\Omega + \frac{V_{\theta i}}{RS_i}\right) & G_{3i} & 0 & 0 & -G_{1i} \frac{P_{\theta i}}{RS_i} & 0 & 0 & 0 \\ 0 & 0 & G_{3i} & G_{1i}\left(-\Omega + \frac{V_{\theta i}}{RS_i}\right) & 0 & 0 & 0 & G_{1i} \frac{P_{\theta i}}{RS_i} \\ 0 & 0 & G_{1i}\left(\Omega - \frac{V_{\theta i}}{RS_i}\right) & G_{3i} & 0 & 0 & -G_{1i} \frac{P_{\theta i}}{RS_i} & 0 \\ X_{3i} & \frac{A_{\theta i}}{RS_i} & 0 & 0 & X_{2i} & X_{1i}\left(\Omega + \frac{V_{\theta i}}{RS_i}\right) & 0 & 0 \\ -\frac{A_{\theta i}}{RS_i} & X_{3i} & 0 & 0 & -X_{1i}\left(\Omega + \frac{V_{\theta i}}{RS_i}\right) & X_{2i} & 0 & 0 \\ 0 & 0 & X_{3i} & \frac{A_{\theta i}}{RS_i} & 0 & 0 & X_{2i} & -X_{1i}\left(\Omega - \frac{V_{\theta i}}{RS_i}\right) \\ 0 & 0 & -\frac{A_{\theta i}}{RS_i} & X_{3i} & 0 & 0 & X_{1i}\left(\Omega - \frac{V_{\theta i}}{RS_i}\right) & X_{2i} \end{bmatrix}$$